Supporting Information

Proton Coupled Electron Transfer Process from Functionalized Carbon Dot to Molecular Substrates: Role of pH

Umarfaruk S. Sayyad, [a] Sapna Waghmare, [a] Somen Mondal[a]*

[a]*Institute of Chemical Technology, Mumbai, Marathwada Campus, Jalna, Maharashtra 431203, India.*

1. Material and Method:

1.1. Materials:

Citric acid, ethylenediamine (EDA), sodium dihydrogen phosphate, and sodium phosphate dibasic heptahydrate all were purchased from Sigma Aldrich; 1,4-Benzoquinone was purchased from Sisco Research Lab Pvt. Ltd., cyclohexanone was purchased from molychem. All chemicals were research grade and were used without further purification. All experiments were carried out in ultrapure deionized water.

1.2. Synthesis:

1.2.1. Synthesis of C-Dot-COOH:

The carboxylic group enriches C-Dots, 1 g of citric acid was mixed with 50 ml of ethylenediamine (EDA) (small amount) and dissolved in 5 mL of deionized water to make C-Dots-COOH. Then,

the mixture was placed in a microwave and heated to 180°C for 20 minutes at 150 watts. The resulting solution became colorless to yellowish. After that, the excess water was removed using a rotary evaporator, which yielded a gel-like substance. The product was washed with acetone and methanol and continued the same step 4-5 times. [1]

1.2.2. Synthesis of C-Dot-NH_2:

The amine-enriched C-Dot-NH_2 was prepared from 1 g of citric acid and 1 mL of EDA to serve as the precursor of the NH_2 group. The mixture of citric acid and EDA was dissolved in 5 mL of deionized water and transferred to a vial for microwave synthesis. After that, the reaction mixture was heated at 180 °C, 50 watts of power, and continued for 20 minutes. Finally, the solution became dark brown. Finally, the product was washed with acetone and methanol and continued the same step 4-5 times.[1]

1.3. Instrumentation and Sample Characterization:

1.3.1. Transmission Electron Microscopy and HRTEM Analysis:

The size and shape of the synthesized materials were examined using the JEOL JEM 2100F Field Emission Gun-Transmission Electron Microscope (TEM) at 200 kV. To prepare the sample for TEM analysis, a methanolic dispersion of the sample was drop-casted onto a carbon-coated copper grid measuring 200 mesh. The sample was left to dry overnight under a vacuum.

1.3.2. X-Ray Diffraction Analysis:

The material's crystal structure was analyzed using the BRUKER-D8 ADVANCE DA VINCI X-Ray Diffractometer and copper K-α radiation of wavelength 1.5406 Å. C-Dots were drop-casted on glass slides and dried under vacuumed desiccator for 24 hours.

1.3.3. Fourier Transform Infrared Spectroscopy:

FTIR spectra were recorded using a JASCO FT/IR 6600 spectrometer on the zinc sulfide crystal using ATR mode at room temperature.

1.3.4. UV-Visible Spectra and PL Spectra:

To clarify the optical properties, we measured the absorbance of all C-Dots on a Shimadzu UV-2600i UV-Visible spectrophotometer and recorded the steady-state fluorescence spectra on a JASCO spectrofluorometer using water as a solvent.

1.3.5. Raman Spectroscopy:

The In Via Raman Microscope was utilized to capture the Raman spectra of each C-Dot. A high-power near-IR diode laser with 300 mW output at 785 nm (air-cooled) served as the excitation light source. To ensure precision, an integral narrow bandpass filter was externally mounted on a laser kinematic baseplate.

1.3.6. Time-Correlated Single Photon Counting Measurement:

Time-resolved fluorescence quenching analysis was carried out on TCSPC with the Delta-pro TCSPC lifetime system from Horiba Scientific. The samples were excited using 390 nm LED as a light source and the emission was monitored the emission at 440 nm using a cut-off filter. The instrument response function (IRF) was recorded as 1.2 ns. Initially, the IRF was measured using a milk solution in water. All C-Dots were dissolved in water, and the acquired data was fitted using EZ time software.[2] The average lifetime was calculate using the following equation:

$$\tau_{avg} = \sum \alpha_i \tau_i / \sum \alpha_i \qquad \text{..... S1}$$

1.4. Electrical Study:

1.4.1. Electrochemical Measurements:

To understand the PCET reagent properties of the C-Dots, the cyclic voltammetry experiment was performed using three electrode system where the glassy carbon electrode functionalized in 0.5 M sulfuric acid was used as a working electrode, the SCE (Ag/AgCl) containing 3M KCl as a supporting electrolyte was used as a reference and platinum wire was used as a counter electrode on Metrohm Autolab electrochemical workstation. Initially, 2 mg C-Dots were dissolved in a phosphate buffer solution (PBS). The CV analysis was carried out using homogenous electrolysis at a scan rate of 100 mV/s in the potential window of -1.5 to 1.5 V. The obtained potential against SCE was converted to against SHE by the addition of 197 mV in the potential against SCE.

According to the Nernst equation, (**eq. S2**) the potential (E) for molecular 2e/2p transfer shifts by 28 mV. The redox reaction at equilibrium is given in equation (**eq. S3**). The oxidation and reduction of C-Dots with pH can be written as follow the Nernst equation (**eq. S4**)[3]:

$$E_{\left(X + 2e - + \frac{2H^+}{XH_2}\right)} = E° - 28\ mV - log\frac{[XH_2]}{[X]} - 0.059\,V \times pH \quad \text{..... (S2)}$$

$$CDots + e + H^+ \rightleftharpoons CDots\bullet e\bullet H^+ \quad \text{.....(S3)}$$

$$E_{CDot\left(\frac{ox}{red}\right)} = E° - 28\ mV - log\frac{[CDot\,]red}{[CDot\,]ox} - 0.059\,V \times pH \text{.....} \quad \text{... (S4)}$$

1.5. Photocatalytic activity:

The photoinduced PCET reaction was confirmed using photocatalytic conversion from 1,4-Benzoquinone (BQ) to hydroxyquinone (H_2Q) in the presence and absence of C-Dots. The mixture

of 0.5 µL (100 mg/mL) C-Dots and 0.1 mL 1,4-Benzoquinone solution (0.05 mM) was added in 2 ml PBS solution in a quartz cuvette. After that, nitrogen gas flowed through the reaction mixture for 20 min. Finally, the inert reaction mixture was irradiated with the 365 nm ultra violate light,

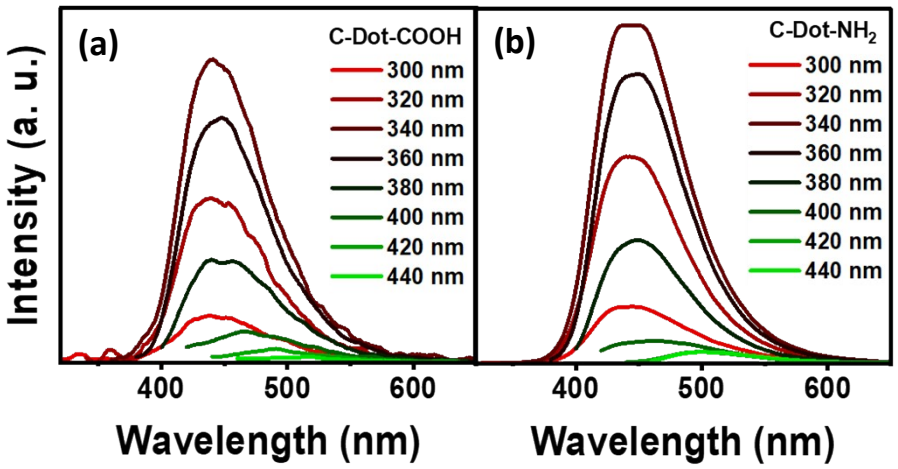

and the absorbance was measured by the 2 min interval.

Figure S1: Excitation wavelength-dependent emission spectrum of (a) C-Dot-COOH (b) C-Dot-

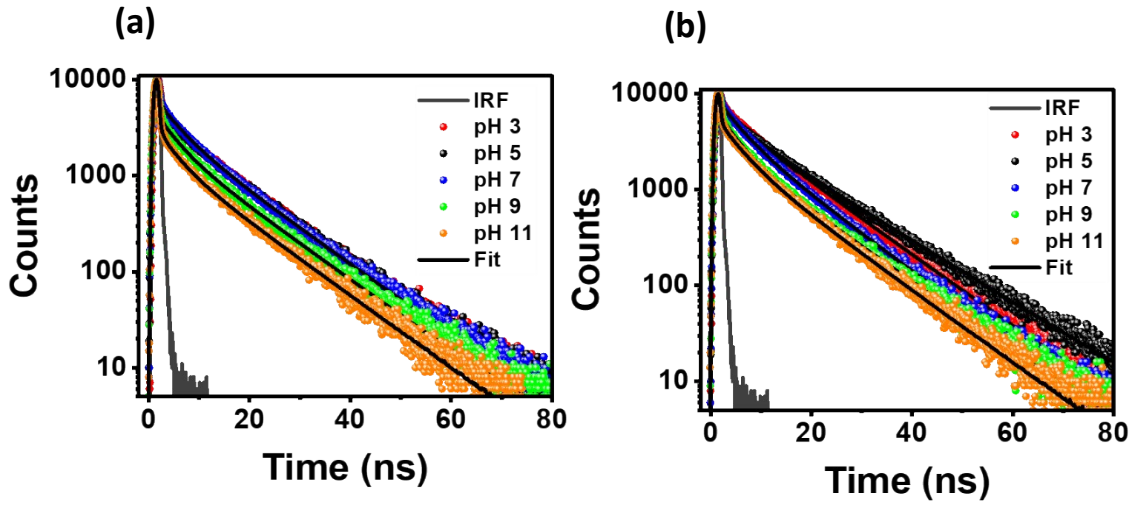

NH_2 respectively.

Figure S2: pH-dependent Time-resolved fluorescence spectrum for (a) C-Dot-COOH (b) C-Dot-NH_2.

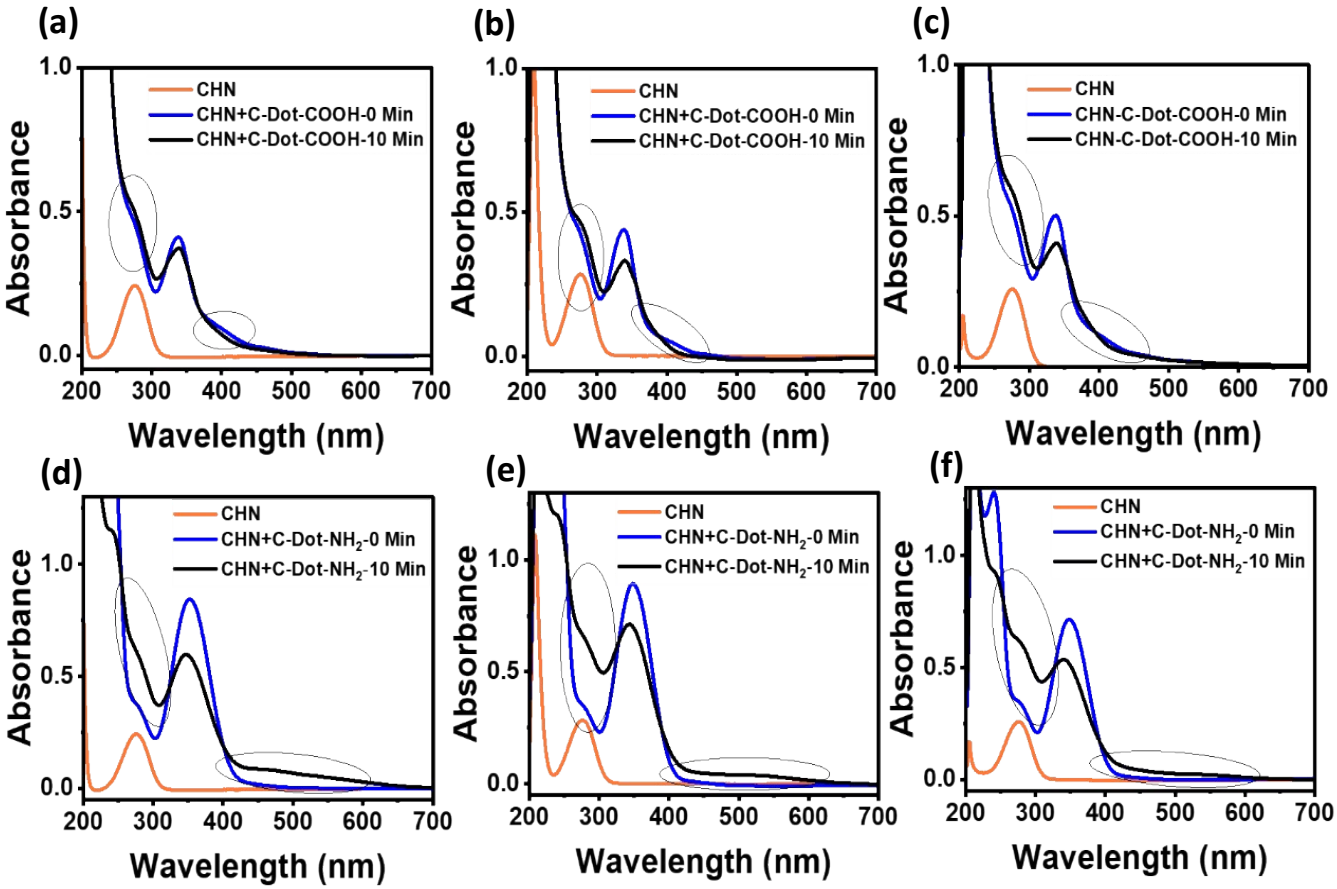

Figure S3: Absorbance spectrum of photoreduction form CHN to Cyclohexanol in presence of C-Dot-COOH at (a) pH=3, (b) pH=7, (c) pH=9 and C-Dot-NH_2 at (d) pH=3, (e) pH=7, and (f) pH=9.

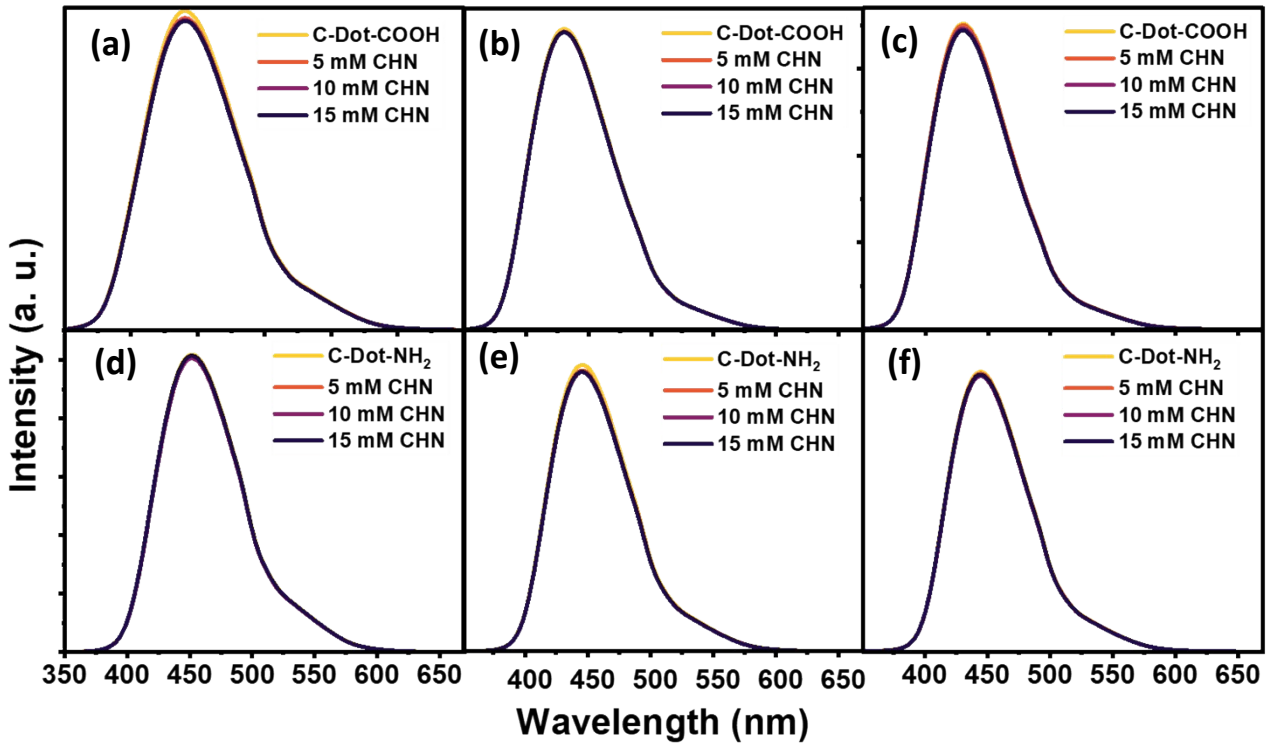

Figure S4: Steady state PL study of C-Dot-COOH at (a) pH=3 (b) pH=7 and (c) pH=9 and C-Dot-NH_2 at (d) pH=3, (e) pH=7, and (f) pH=9 with the addition of CHN.

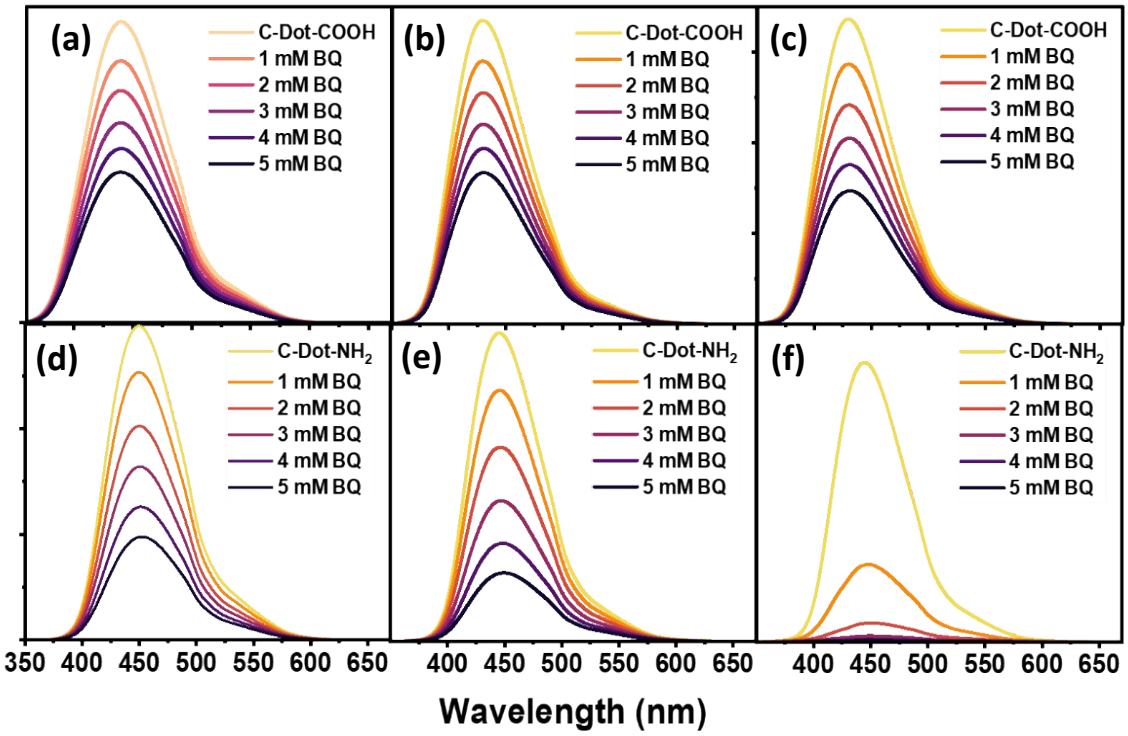

Figure S5: Steady state PL quenching of C-Dot-COOH at (a) pH=3 (b) pH=7 and (c) pH=9 and C-Dot-NH_2 at (d) pH=3, (e) pH=7, and (f) pH=9 with the addition of BQ upto 5mM.

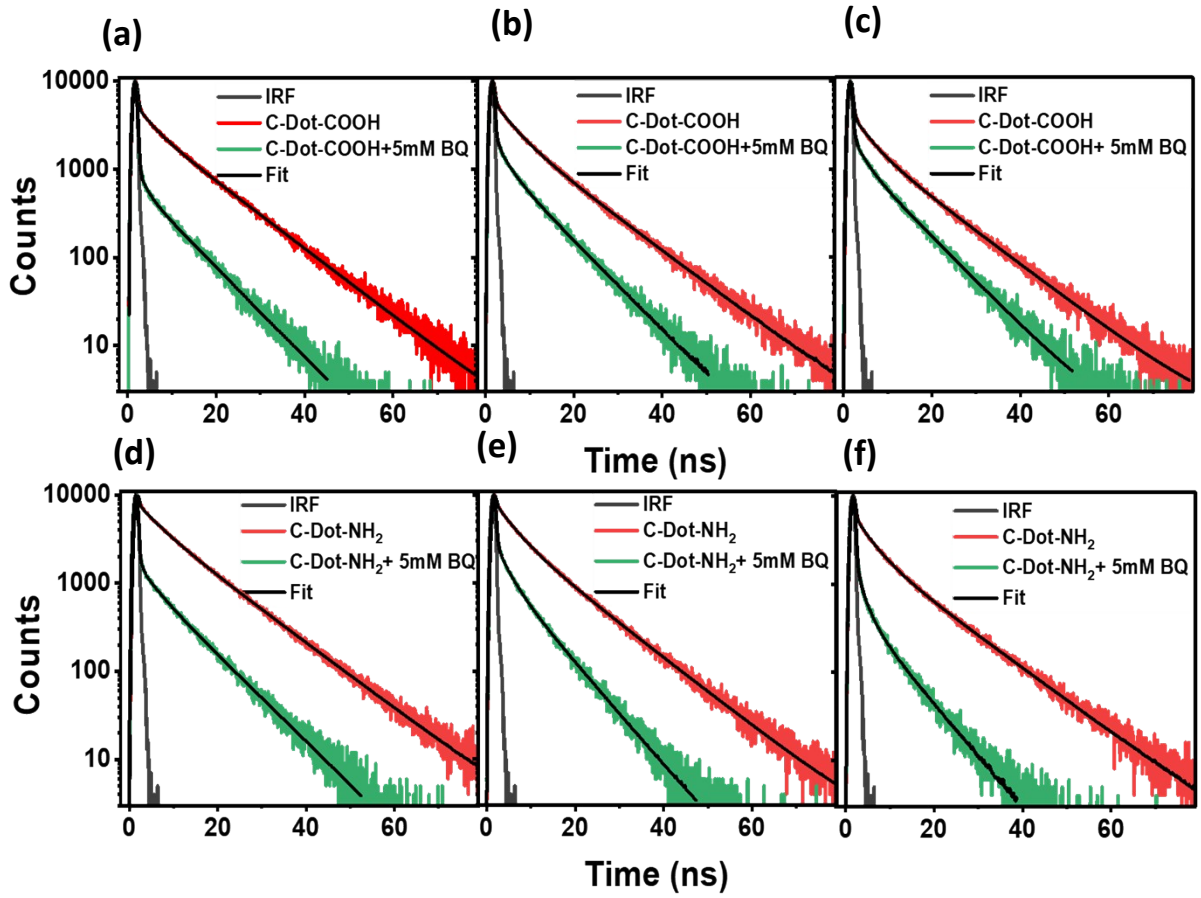

Figure S6: Time-resolved PL study of C-Dot-COOH at (a) pH=3 (b) pH=7 and (c) pH=9 and C-Dot-NH_2 at (d) pH=3, (e) pH=7, and (f) pH=9 with the addition of BQ.

Table S1: Fitting time constants for the kinetics at 440 nm of C-Dot-COOH after exciting the sample at 340 nm using TCSPC mode at different mode.

C-Dot-COOH							
pH	**τ_1 (ns)**	**B_1 (%)**	**τ_2 (ns)**	**B_2 (%)**	**τ_3(ns)**	**B_3 (%)**	**χ^2**
3	<1	15.48	3.26	11.21	11.34	73.31	1.05
5	<1	17.62	3.52	11.04	11.54	71.34	1.04
7	<1	15.06	4.13	20.74	11.56	64.2	1.11
9	<1	21.94	3.55	17.64	11.45	60.42	1.09
11	<1	34.73	3.51	14.86	11.40	50.42	1.15

Table S2: Fitting time constants for the kinetics at 440 nm of C-Dot-NH_2 after exciting the sample at 340 nm using TCSPC mode at different pH.

C-Dot-NH_2							
pH	**τ_1 (ns)**	**B_1 (%)**	**τ_2 (ns)**	**B_2 (%)**	**τ_3(ns)**	**B_3 (%)**	**χ^2**
3	<1	6.93	4.63	14.74	11.59	78.33	1.09
5	<1	7.8	4.88	11.39	11.375	80.81	1.06
7	<1	7.75	4.06	24.07	11.13	68.19	1.10
9	<1	16.65	3.75	23.54	11.76	59.81	1.13
11	<1	19.5	4.101	22.04	11.34	58.46	1.13

BQ (mM)	τ_1 (ns)	B_1 (%)	τ_2 (ns)	B_2 (%)	τ_3(ns)	B_3 (%)	χ^2
0	<1	15.48	3.26	11.21	11.34	73.31	1.05
1	<1	37.91	2.42	7.22	10.31	54.88	1.13
2	<1	49.3	2.35	6.42	9.87	44.28	1.10
3	<1	56.58	1.97	5.2	9.20	38.22	1.12
4	<1	63.72	1.88	4.12	8.61	32.16	1.23
5	<1	68.23	1.65	4.71	8.47	27.05	1.22

Table S3: Time constants for the kinetics at 440 nm of C-Dot-COOH after the excitation at 390 nm with the progressive addition of BQ in PBS 3.

Table S4: Time constants for the kinetics at 440 nm of C-Dot-COOH after the excitation at 390 nm with the progressive addition of BQ in PBS 7.

BQ (mM)	τ_1 (ns)	B_1 (%)	τ_2 (ns)	B_2 (%)	τ_3(ns)	B_3 (%)	χ^2
0	<1	15.06	4.13	20.74	11.56	64.2	1.11
1	<1	24.35	3.82	18.38	10.89	57.27	1.10
2	<1	32.75	3.51	15.77	10.28	51.48	1.10
3	<1	35.43	3.28	14.98	9.67	49.6	1.14
4	<1	41.84	2.88	12.23	9.05	45.93	1.08
5	<1	50.41	2.62	10.32	8.54	39.27	1.07

BQ (mM)	τ_1 (ns)	B_1 (%)	τ_2 (ns)	B_2 (%)	τ_3(ns)	B_3 (%)	χ^2
0	<1	21.94	3.55	17.64	11.45	60.42	1.09
1	<1	25.37	3.48	17.07	10.71	57.56	1.02
2	<1	28.16	3.22	15.92	9.98	55.92	1.03
3	<1	35.98	2.73	12.96	9.32	51.06	1.08
4	<1	38.97	2.84	13.27	9.12	47.76	1.13
5	<1	43.5	2.38	10.8	8.54	45.7	1.26

Table S5: Time constants for the kinetics at 440 nm of C-Dot-COOH after the excitation at 390 nm with the progressive addition of BQ in PBS 9.

BQ (mM)	τ_1 (ns)	B_1 (%)	τ_2 (ns)	B_2 (%)	τ_3(ns)	B_3 (%)	χ^2
0	<1	6.93	4.63	14.74	11.59	78.33	1.09
1	<1	13.68	4.38	13.84	11.01	72.49	1.04
2	<1	26.77	3.79	9.96	10.26	63.27	1.00
3	<1	36.36	3.24	7.35	9.54	56.29	1.03
4	<1	49.8	3.52	6.54	9.20	43.66	1.08

5	<1	55.69	3.48	6.51	8.92	37.81	1.02

Table S6: Time constants for the kinetics at 440 nm of C-Dot-NH_2 after the excitation at 390 nm with the progressive addition of BQ in PBS 3.

BQ (mM)	τ_1 (ns)	B_1 (%)	τ_2 (ns)	B_2 (%)	τ_3(ns)	B_3 (%)	χ^2
0	<1	7.75	4.06	24.07	11.13	68.19	1.10
1	<1	12.12	4.00	24.17	10.72	63.71	1.08
2	<1	19.93	3.46	20.64	9.72	59.43	1.16
3	<1	26.61	3.23	19.61	8.95	53.78	1.08
4	<1	39.1	3.04	18.3	8.27	42.6	1.03
5	<1	46.68	2.61	15.15	7.44	38.18	1.19

Table S7: Time constants for the kinetics at 440 nm of C-Dot-NH_2 after the excitation at 390 nm with the progressive addition of BQ in PBS 7.

BQ (mM)	τ_1 (ns)	B_1 (%)	τ_2 (ns)	B_2 (%)	τ_3(ns)	B_3 (%)	χ^2
0	<1	16.65	3.75	23.54	11.76	59.81	1.13
1	<1	19.54	3.70	26.67	10.82	53.79	1.19

Table S8: Time constants for the kinetics at 440 nm of C-Dot-NH_2 after the excitation at 390 nm with the progressive addition of BQ in PBS 9.

2	<1	36.73	3.13	24.61	8.89	38.66	1.15
3	<1	52.88	2.60	18.35	7.62	28.78	1.19
4	<1	59.89	2.24	14.68	7.39	25.44	1.26
5	<1	68.51	1.94	12.16	7.09	19.34	1.19

Table S9: Comparison of PCET process with some reported carbon-based materials.

Sr. No.	System	Study done and outcomes	Reference
1	Graphite conjugated organic acid catalyst (GCC)	• Catalyst on GCC electrode • Study the electrochemical PCET process • Calculated thermodynamical parameters	31
2	Graphite conjugated organic acid catalyst (GCC)	• Catalyst on GCC electrode • Computational study • Thermodynamical evidence of PCET process	32
4	Graphene nanoribbons coupled on GCE	• Material conjugated on GCC electrode • $4e^-/4H^+$ process is favourable at low pH • $2e^-/2H^+$ process is favourable at high pH • Study the electrochemical PCET process	33
3	N-Doped Graphene oxide	• Computational study • Photocatalytic Water Splitting	34
5	Aqueous C-Dots	• Nanomaterial • Calculation of ground state and excited state pk_a • Investigated the corelation between pk_a and PCET • Study the electrochemical PCET process • Thermodynamical evidence of PCET process via BDFE calculation • Optical study to follow the electron transfer dynamics in PCET kinetics • Direct proof of PCET process via	**This Work**

		photoreduction of BQ and CHN	

References

1 S. Mondal, A. Yucknovsky, K. Akulov, N. Ghorai, T. Schwartz, H. N. Ghosh and N. Amdursky, *J. Am. Chem. Soc.*, 2019, **141**, 15413–15422.

2 U. S. Sayyad, H. Bhatt, H. N. Ghosh and S. Mandal, *Nanoscale*, 2024, **16**, 8143-8150.

3 J. L. Peper, N. E. Gentry, B. Boudy and J. M. Mayer, *Inorg. Chem.*, 2022, **61**, 767–777.

4 M. N. Jackson, M. L. Pegis and Y. Surendranath, *ACS Cent. Sci.*, 2019, **5**, 831–841.

5 R. E. Warburton, P. Hutchison, M. N. Jackson, M. L. Pegis, Y. Surendranath and S. Hammes-Schiffer, *J. Am. Chem. Soc.*, 2020, **142**, 20855–20864.

6 F. Weber, J. C. Tremblay and A. Bande, *J. Phys. Chem. C.*, 2020, **124**, 26688–26698.

7 M. R. Zoric, E. J. Askins, X. Qiao and K. D. Glusac, *ACS Appl. Electron. Mater.,* **2021**, 3, 854–860.